OncoTargets and Therapy

Dovepress
open access to scientific and medical research

Open Access Full Text Article

ORIGINAL RESEARCH

Synergistic effect of meta-tetra(hydroxyphenyl) chlorin-based photodynamic therapy followed by cisplatin on malignant Hep-2 cells

This article was published in the following Dove Press journal:
OncoTargets and Therapy

Kai Xue[1]
Yi-Nan Wang[2]
Xue Zhao[1]
Hong-Xin Zhang[3]
Dan Yu[1]
Chun-Shun Jin[1]

[1]Department of Otolaryngology-Head and Neck Surgery, The Second Hospital of Jilin University, Changchun 130041, People's Republic of China; [2]Department of Gynecology and Obstetrics, The Second Hospital of Jilin University, Changchun 130041, People's Republic of China; [3]Changchun Institute of Optics, Fine Mechanics & Physics, Chinese Academy of Sciences, Changchun 130033, People's Republic of China

Purpose: Tumor drug resistance limits the response to chemotherapy. Interestingly, sequential combination therapy enhances the anticancer efficacy of drugs like cisplatin (CDDP) via synergistic effects. We assayed the synergistic effects of combined photodynamic therapy programmed death receptor-ligand 1 (PDT) and chemotherapy in malignant Hep-2 cells.

Methods: In the cultured Hep-2 cells, meta-tetra(hydroxyphenyl)chlorin (m-THPC) and CDDP were administered separately or in combination. The cellular viability and apoptosis were assessed, accompanied by measurement of the expression of Bax, Bcl-2, ATG-7, and LC3 (LC3-I and LC3-II). Additionally, nuclear chromatin changes, drug retention, and PD-L1 expression were further investigated following different treatments.

Results: The sequential treatment significantly diminished cell viability and induced cell apoptosis, in consistency with the usage of single therapeutic strategies, as reflected by an increase in Bax expression and decrease of Bcl-2 expression. Moreover, ATG-7 and LC3-II /LC3-I ratio were reduced after administration of the sequential treatment. Synergetic effect of nuclear chromatin configuration, negative effects of cellular drug retention, and a decrease in PD-L1 expression were observed following the sequential treatment.

Conclusion: The application of sequential treatment of PDT in combination with chemotherapy offers a promising therapeutic option for cancer treatment, by regulating the PD-L1 expression, autophagy, and non-mitochondrial pathways.

Keywords: photodynamic therapy, sequential treatment, chemotherapy, PD-L1, Hep-2 cell

Introduction

Chemotherapy is the first-line therapeutic modality for the treatment of cancer. However, the increasing drug resistance confers the efficacy of ongoing chemotherapy due to various intrinsic or acquired mechanisms, including tumor heterogeneity, increased expression of drug efflux transporters, genetic or epigenetic changes induced by stress from metabolism and tumor microenvironment, detoxification of cytotoxic agents, increased autophagy, and programmed death receptor-ligand 1 (PD-L1) expression, causing relapse or even metastasis.[1–6] In an attempt to overcome the barrier of chemo-resistance, the combination approach of using different chemotherapeutic agents or modalities has been explored in order to target different key signal transduction pathways and to enhance the overall therapeutic efficacy via synergistic or additive effects.[7,8]

Photodynamic therapy (PDT) is a type of therapeutic treatment that targets and destroys malignant cancer tissues upon stimulation of multiple chemical reactions by

Correspondence: Dan Yu; Chun-Shun Jin
Department of Otolaryngology-Head and Neck Surgery, The Second Hospital of Jilin University, No. 218, Ziqiang Street, Nanguan District, Changchun 130041, Jilin Province, People's Republic of China
Tel +86 431 8113 6796
Email yudan19792003@sina.com; jchunshun@126.com

submit your manuscript | www.dovepress.com
DovePress
http://doi.org/10.2147/OTT.S198422

administration of a photosensitizer under direct exposure of light.[9–12] PDT has been clinically approved which led to its extensive use as a therapeutic strategy for various premalignant and malignant types of cancers worldwide for years.[13] In addition, recent evidence supports the use of PDT in combination with several kinds of chemotherapeutic drugs for better prognosis of patients. The additive effects of PDT have been observed along with the adverse reactions that might arise while conducting this procedure.[14,15] Previous studies have demonstrated increased apoptosis and autophagy as the driving factors for achieving superior efficacious during the treatment with a combination therapy of chemotherapeutic agents and PDT.[16,17] Moreover, the deleterious side effects on host tissues due to a combination of PDT and chemotherapeutic therapy can be reduced or controlled by using smaller doses of chemotherapeutic agents.[18]

Existing literature has highlighted the efficacy of the combination use of chemotherapy and PDT in a concurrent way, and the efficacy of sequential strategy in clinical practice and the co-treatment of chemotherapy and PDT still requires further study. Therefore, the following study was planned to investigate the use of sequential modality with meta-Tetra (hydroxyphenyl) chlorin (m-THPC)-based PDT followed by cisplatin (CDDP)-based chemotherapy in the cancer cell line (Hep-2) and the synergistic efficacy and the potential mechanisms responsible for this combination therapy.

Materials and methods

Ethical statement

This article does not contain any studies with human participants or animals performed by any of the authors.

Cell culture

Hep-2 cells (ATCC® CCL-23™, VA, USA) were grown in total DMEM culture medium (Hyclone, UT, USA) containing 10% fetal bovine serum (TMS-013-B, Merck Millipore, Darmstadt, Germany), penicillin (100 units/mL, 516104, Merck Millipore, Darmstadt, Germany) and streptomycin (100 µg/mL, 516104, Merck Millipore, Darmstadt, Germany) at 37°C in humid conditions of 5% CO_2 in an incubator (Heracell 240i, ThermoFisher, Rochester, NY, USA). Figure S1 represented the experimental procedure.

Cellular viability with m-THPC and PDT

Hep-2 cells were cultured in 96-well plates (Corning, NY, USA) in 200 µL of total culture medium at a concentration of 1×10^4 cells/well. Subsequently, the cells were divided into six groups with further six sub-groups in each group. The cells in these six groups were then exposed to the photosensitizer m-THPC (HY-16488, MedChem Express, NJ, USA) at concentrations of 0.1, 0.5, 1, 2, 5, and 10 µM, respectively, and incubated in conditions devoid of light at 37°C with 5% CO_2 in an incubator for 24 hrs after seeding. After 24 hrs, the cells in six sub-groups were exposed to laser of a wavelength of 650 nm (Changchun Institute of Optics, Fine Mechanics & Physics, Chinese Academy of Sciences, Changchun, China) with energy delivered at variable doses (0, 0.1, 0.5, 1, 2, and 5 J/cm^2), respectively. The control group was administered no treatment and was only cultured in total culture medium. Upon three rinses with phosphate buffer saline (PBS), fresh culture medium was added to the cells. After 24 hrs, 3-(4, 5-dimethylthiazol-2-yl)-2, 5-diphenyltetrazolium bromide (MTT) assay was performed in order to measure the cellular viability. The experiments on each m-THPC concentration and laser energy dose were performed in triplicates.

Cellular viability with CDDP treatment

Hep-2 cells were cultured in 96-well plates at a concentration of 1×10^4 cells/well in 200 µL of total culture medium. The cells were further divided into six groups. After 48 hrs, CDDP (Yuanye Bio, Shanghai, China) was added into each group at variable concentrations of 2, 5, 10, 20, 50, and 100 µM, respectively. The Hep-2 cells in the control group were cultured with total culture medium without any treatment. Cellular viability was measured by means of MTT assay at 24 hrs post treatments. Experiments on each CDDP concentration were performed in triplicates.

MTT assays

The cells were cultured in 96-well plates (3,000 cells/well). Upon completion of the culture, MTT solution (10 mg/mL, Sigma, St Louis, MO, USA) was added to each well. The viability of the cells was assessed using a microplate reader at a wavelength of 570 nm.

Investigation of sequential treatment with PDT followed by CDDP

Treatment groups were set up as follows:

Control group

Hep-2 cells were cultured for 48 hrs in 200 µL of total culture medium, followed by 3 rinses using PBS, and

addition of 200 μL fresh total culture medium, after which cell culture was conducted for 24 hrs.

PDT group

Hep-2 cells were cultured in a 96-well plate at a concentration of 1×10^4 cells/well in 200 μL of total culture medium. The Hep-2 cells were cultured using m-THPC at the concentration of 0.5 μM for 24 hrs after 24 hrs of seeding, followed by exposure to a 650 nm laser at an energy dose of 2 J/cm^2. Subsequently, the Hep-2 cells were rinsed using PBS 3 times, followed by the addition of 200 μL fresh total culture medium and cell culture. MTT assay was performed for cell analysis after 24 hrs.

CDDP group

Hep-2 cells were cultured in 96-well plates at a concentration of 1×10^4 cells/well in 200 μL of total culture medium. After performing medium replacement with fresh culture medium, CDDP was added at the concentration of 5 μM after 48 hrs of seeding, followed by cell culture for 24 hrs.

PDT + CDDP group

The aforementioned method was repeated for cell culture of the Hep-2 cells. The Hep-2 cells were then cultured using m-THPC at the concentration of 0.5 μM for 24 hrs, after 24 hrs of seeding. Afterward, the Hep-2 cells were exposed to a 650 nm laser at an energy dose of 2 J/cm^2. After 3 rinses with PBS, the cells were cultured in fresh culture medium containing CDDP at a concentration of 5 μM for 24 hrs. All experiments were performed in triplicates.

Flow cytometry analysis

Hep-2 cells were cultured in 6-well plates at a concentration of 2×10^5 cells/well. Following the aforementioned treatments (part of investigation of sequential treatment with PDT followed by CDDP), the Hep-2 cells were collected by performing trypsin detachment, re-suspension in 1× binding buffer from the Dead Cell Apoptosis Kit with FITC-Annexin V and PI (BD Biosciences Pharmingen, San Jose, CA, USA) at a concentration of 1×10^6 cells/mL and stained using the Dead Cell Apoptosis Kit with FITC-Annexin V and PI in strict accordance following the manufacturer's protocol. Coulter Epics XL flow cytometer (Beckman Coulter, Fullerton, CA, USA) was used for analysis of the stained cells.

Western blot analysis

Western blot method was conducted according to the following procedure: Hep-2 cells were plated in 100 mm cell culture dishes at a concentration of 2×10^6 cells/dish, followed by the addition of 100 μL of RIPA lysis buffer for performing lysis in cells of each group. A total of 20 μg of proteins were loaded into each lane for preforming sulfate polyacrylamide gel electrophoresis. Next, the protein was transferred onto polyvinylidene fluoride (PVDF) membranes after which membrane blockade was conducted for 1 hr using 5% non-fat milk in TBST. The membranes were incubated with monoclonal antibodies (Abcam, Cambridge, UK) against human Bax, Bcl-2, ATG-7, LC3 (LC3-I +LC3-II), and β-actin overnight at 4°C with agitation. After 3 rinses with TBST, the membranes were incubated with HRP-conjugated goat anti-mouse or anti-rabbit antibodies (Abcam, Cambridge, UK) at room temperature for 1 hr. Finally, the membranes were developed using a Pico Chemiluminescent (Fisher Scientific, Hampton, NH, USA), and the results were analyzed on a Tanon 5200 Chemiluminescent Imaging System (Tanon, Shanghai, China) based on the luminescence values with β-actin serving as a reference gene.

Hoechst 33258 staining for the observation of nuclear chromatin changes

Hep-2 cells were inoculated into 6-well plates containing sterile cover glasses (Cat. 12-545-83, Fisher Scientific, Hampton, NH, USA) at a concentration of 2×10^5 cells/well. The cells underwent treatment following the aforementioned protocol. After treatment, the cells on coverslips were first stained with Hoechst 33258 (Beyotime, Shanghai, China) in accordance with the manufacturer's protocol. The stained cells were observed under an Olympus IX71 Fluorescence Microscope (Olympus Corporation, Tokyo, Japan).

Confocal laser scanning microscopic analysis of drug retention

For drug retention analysis, Hep-2 cells were inoculated into 6-well plates containing sterile cover glasses at a concentration of 2×10^5 cells/well. The cells underwent the aforementioned treatment protocol with an exception of the use of CDDP, which was replaced with 1,3,5,7-tetramethyl-8-(4-pyridyl)-4,4′-difluorobora-dia-zaindacene labeled Platinum conjugate (BODIPY-Pt) (donated by Prof. Zhigang Xie, State Key Laboratory of Polymer Physics and Chemistry, Changchun Institute of Applied Chemistry, Chinese Academy of Sciences, Changchun, China) at a concentration of 30 μM following the guidelines of Xie's research.[19] Near-infrared fluorescence was exhibited by

BODIPY-Pt, which was observable under confocal laser scanning microscopy. After treatment, the Hep-2 cells on coverslips were stained using Mito Tracker™ Red CMXRos (Fisher Scientific, Hampton, NH, USA) in accordance with the manufacturer's protocol, followed by fixation using 4% paraformaldehyde and a final process of Hochest 33258 counterstaining. The stained Hep-2 cells were then observed and analyzed under the Olympus Fluoview FV1000 Confocal Laser Scanning Biological Microscope (Olympus Corporation, Tokyo, Japan).

In an attempt to estimate complete cell fluorescence, the cell boundary was identified for confocal slices by a consistent protocol. First, a rough polygonal region encompassing the whole cell (with an effective edge to include the whole cell in all sections) was designated on one of the middle sections. Next, a threshold operation was performed to obtain the binary image. Because of the non-uniformity of fluorescence distribution and the complexity of morphology, some areas of cells were designated as "holes" (clusters of black pixels surrounded by white pixels) after thresholding. Since subsequent image processing must be performed on cells representing adjacent regions, morphological operation of "filling holes" was performed, followed by "opening" (smoothing) of the cell boundary to obtain the final image, I_F. The final image was binary, which added the fluorescence values of the pixels on the original confocal slice, which became white pixels in I_F, to obtain the total fluorescence in the cell area on the slice. The calculated total fluorescence values of each section were added in an attempt to evaluate the overall fluorescence of the whole cell.

Reverse transcription quantitative polymerase chain reaction (RT-qPCR) analysis of PD-L1 expression

Total RNA was isolated from each sample using the RNeasy® Mini kit (Qiagen, Valencia, CA, USA). cDNA was synthesized and RT-qPCR was performed using the EvoScript Universal cDNA Master (Roche, Basel, Switzerland) on LightCycler® 480 Instrument II (Roche, Basel, Switzerland) with primers for PD-L1 (forward: 5′-TGCAGGGCATTCCAGAAAGA-3′, reverse: 5′-TGCAGCCAGGTCTAATTGTTTT-3′) and β-actin (forward: 5′-ATTGGCAATGAGCGGTTC-3′, reverse: 5′-TAGCACAGCCTGGATAGCAA-3′) genes. The reaction system RT-qPCR was set as follows: pre-incubation at 95°C for 30 s, 45 cycles consisting of 5 s at 95°C and 30 s at 60°C, followed by the cooling program at 40°C for 30 s.

Statistical analysis

The statistical data were analyzed using the SPSS version 23.0 software (SPSS Inc, IL, USA). The data were analyzed by applying the Kolmogorov–Smirnov (K-S) method, and they all conformed to normal distribution. Student's *t*-tests were used for numerical data analysis. The p values less than 0.05 were considered to be statistically significant. All plots were developed using the GraphPad Prism 6 software (GraphPad, San Diego, CA, USA). The IC_{50} of drugs was calculated by means of the CalcuSyn version 2.0 software (BIOSOFT, FCE, UK). The results of immunofluorescence were analyzed using the Image-Pro Plus software (Media Cybernetics, Silver Spring, MD, USA). The Western blots were analyzed using Image J (https://imagej.nih.gov/ij/index.html).

Results

Concentration determination of m-THPC, CDDP, and laser energy dose for sequential treatment

The independent use of various concentrations of m-THPC illustrated no evident difference in terms of cell growth after 24 hrs of culture. At a fixed laser energy dose, a decrease in cell viability was observable with an increase of m-THPC concentration, as shown in Figure 1A. When the energy dose of laser was 2 J/cm^2, the IC_{50} of m-THPC was 0.74 μM. According to Palumbo's study,[20] 0.5 μM of m-THPC and 2 J/cm^2 energy dose of laser for PDT were selected for subsequent treatment. According to Figure 1B, 5 μM CDDP was chosen as the following experimental condition, due to a similar effect on cell viabilities as that of 0.5 μM m-THPC and 2 J/cm^2.

Sequential treatment with PDT followed by CDDP significantly decreased cell viability compared to single treatment

As shown in Figure 2, a significant decrease was evident in the cell viability following the sequential treatment of modality as compared to individual treatments. The results of flow cytometry analysis were depictive of Hep-2 cell apoptosis due to CDDP; however, PDT resulted in necrosis (Figure 3). The apoptosis rate from the sequential

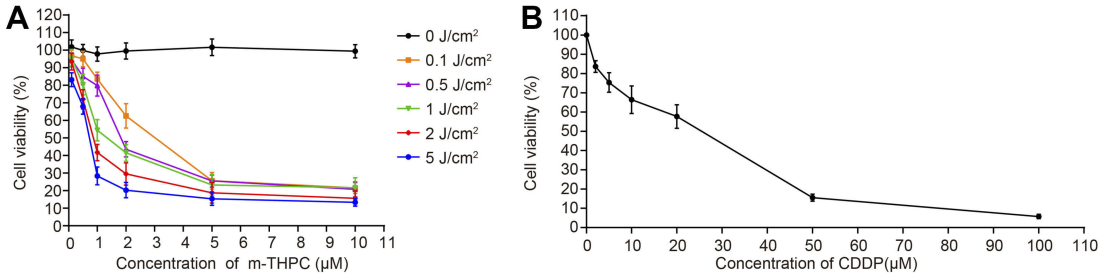

Figure 1 The cell viabilities of various laser dose and concentrations of m-THPC and CDDP using MTT assay. Both (**A**) and (**B**) showed that the cell growth decreased as the dose of laser and concentrations of m-THPC and CDDP increased. Values are expressed as mean percentage ± SD, and the experiment was repeated in triplicate.
Abbreviations: m-THPC, meta-Tetra (hydroxyphenyl) chlorin; CDDP, cisplatin; MTT, 3-(4,5-Dimethylthiazol-2-yl)-2,5-diphenyltetrazolium bromide.

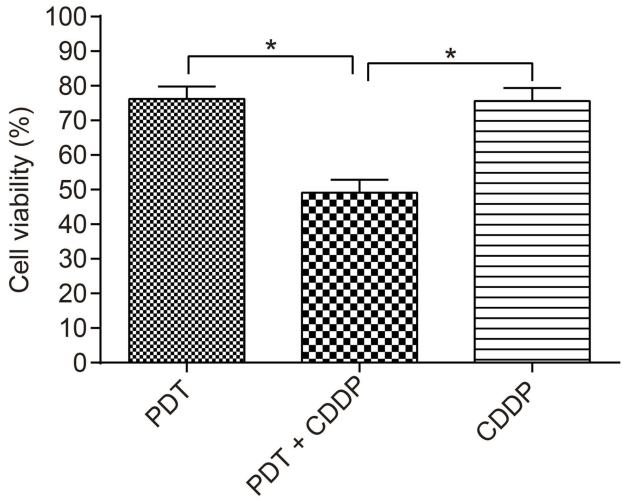

Figure 2 MTT assay resulted from different treatment groups. The cell viability of the PDT+CDDP group was significantly decreased compared to PDT and CDDP groups. Values are expressed as the mean percentage ± SD, and the experiment was repeated in triplicate (*$p<0.05$).
Abbreviations: PDT, photodynamic therapy; CDDP, cisplatin; MTT, 3-(4,5-Dimethylthiazol-2-yl)-2,5-diphenyltetrazolium bromide.

treatment group was higher than that from the PDT treatment group, while no difference was observed in the apoptosis rate compared with CDDP treatment. On the contrary, cell necrosis rate from the sequential treatment group was higher than that from the CDDP group, but no difference was observed in comparison with the PDT group. As shown in Figure 3D, the total cell death was higher in the sequential treatment group than in the single treatment groups.

Western blot analysis results were indicative of an elevated Bax expression after sequential treatment, as shown in Figure 4A and B. The expression of Bcl-2 after sequential treatment had decreased in comparison with the PDT treatment, as shown in Figure 4A and C. The aforementioned results signified that the sequential treatment resulted in the enhancement of Hep-2 cell apoptosis.

Sequential treatment with PDT followed by CDDP reduced autophagy of Hep-2 cells

As illustrated in Figure 5A and B, the sequential treatment resulted in a significant reduction of ATG-7 level in comparison with PDT or CDDP treatment individually. The LC3-II/LC3-I ratio of the sequential treatment group was reduced compared with the PDT group, but these findings were contradicting in the CDDP group, as shown in Figure 5A and C. These results demonstrated that the sequential treatment resulted in reduced autophagy levels.

Sequential treatment with PDT followed by CDDP resulted in the synergetic destruction of nuclear chromatin

The effects of PDT and CDDP treatments on chromatin of Hep-2 cells were evident after performing Hoechst 33258 staining (Figure 6). In the control group, about 2% of the cell nuclei were deeply stained with a dense dye showing light color with regular configurations while uniform blue nuclei of the other cells were observed under a fluorescence microscope. However, CDDP treatment (35%) resulted in superior extensive destruction of nuclear chromatin in comparison with PDT treatment (30%) individually. In the PDT +CDDP group, about 80% of the cells had irregularly fragmented nuclei which were stained by dense dye showing light color. Sequential modality highly affected nuclear chromatin Hep-2 cells, with more intensive nuclear fragmentations and irregularities, as illustrated in Figure 6.

Sequential treatment with PDT followed by BODIPY-Pt had negative effect on cellular drug retention

Previous research has highlighted that BODIPY-Pt had an effect on mitochondria. Therefore, we examined the changes

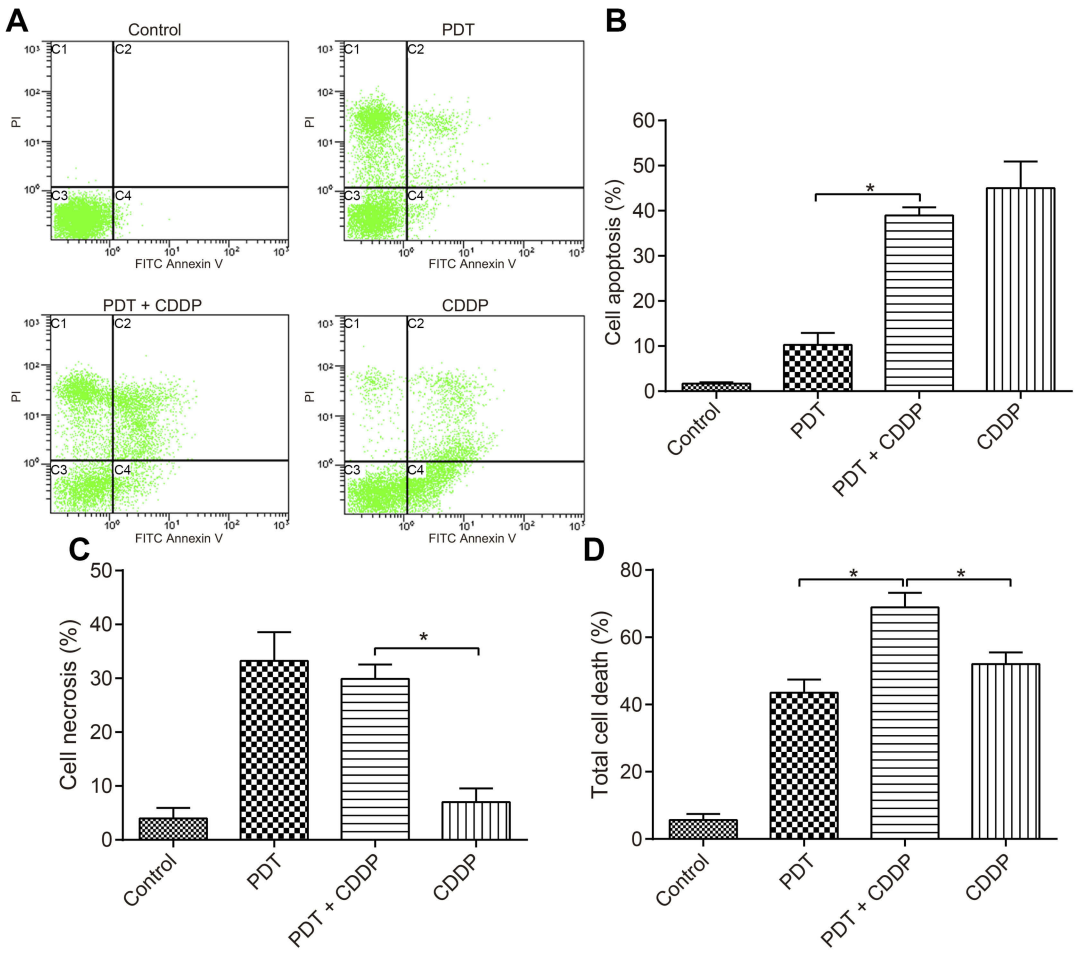

Figure 3 Flow cytometry analysis of percentages of necrotic and apoptotic cells in different treatment groups. Values are expressed as the mean percentage ± SD of triplicates (*p<0.05). (**A**) The various results of Hep-2 cells of different groups. (**B**) The rates of cell apoptosis of different groups. (**C**) The rates of cell necrosis of different groups. (**D**) Total cell death of PDT+CDDP group was significantly increased compared to both PDT and CDDP groups.
Abbreviations: PDT, photodynamic therapy; CDDP, cisplatin.

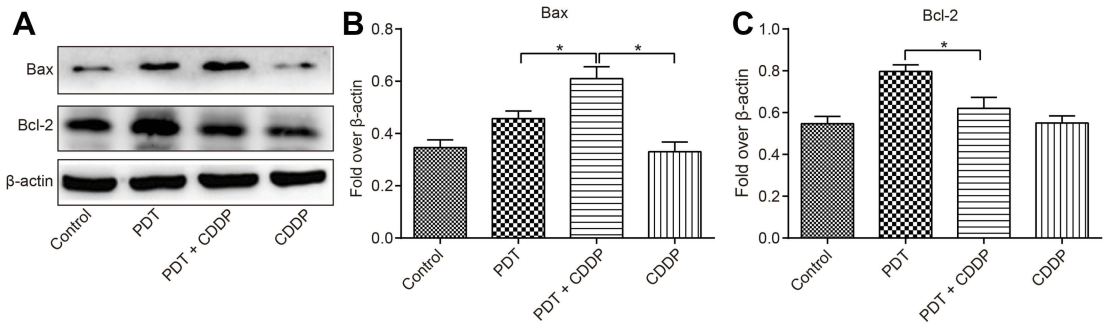

Figure 4 (**A**) Western blot of Bax and Bcl-2 in different groups. β-actin was used as the loading control. (**B**) The expression of Bax in different groups was analyzed. (**C**) The statistical analysis of Bcl-2 expression in different groups. Values are expressed as the mean relative value ± SD, and the experiment was repeated in triplicate (*p<0.05).
Abbreviations: PDT, photodynamic therapy; CDDP, cisplatin.

in the mitochondria following drug treatment. As quantitative analysis of the fluorescence shown (Figure 7A–B), PDT decreased the fluorescence of Mito Tracker red, which meant that PDT could decrease the numbers of mitochondria. Decreased BODIPY fluorescence flagged that it could decrease the retention of mitochondria-targeted drugs.

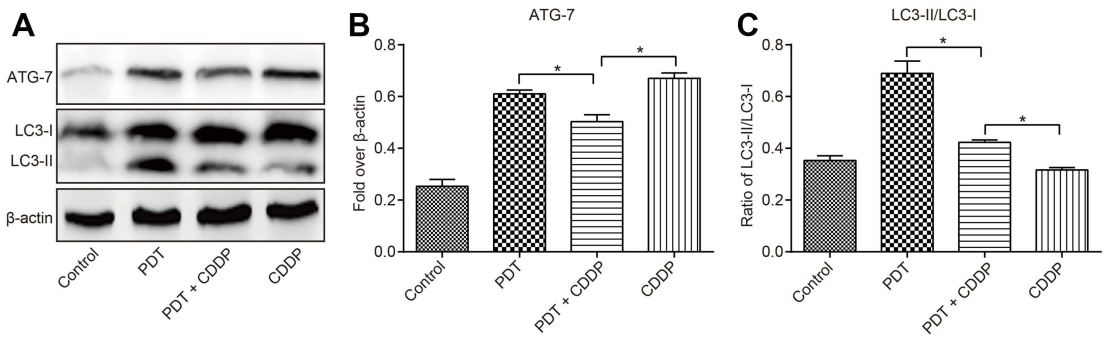

Figure 5 (**A**) Western blot analysis on the expression of ATG-7 and LC3 (LC3-I and LC3-II) from different treatment groups. β-actin was used as the loading control. (**B**) The analysis of expression of ATG-7 in different groups. (**C**) The analysis of ratio of LC3-II/LC3-I in different groups. Values are expressed as the mean relative value±SD, and the experiment was repeated in triplicate (*p<0.05).
Abbreviations: PDT, photodynamic therapy; CDDP, cisplatin.

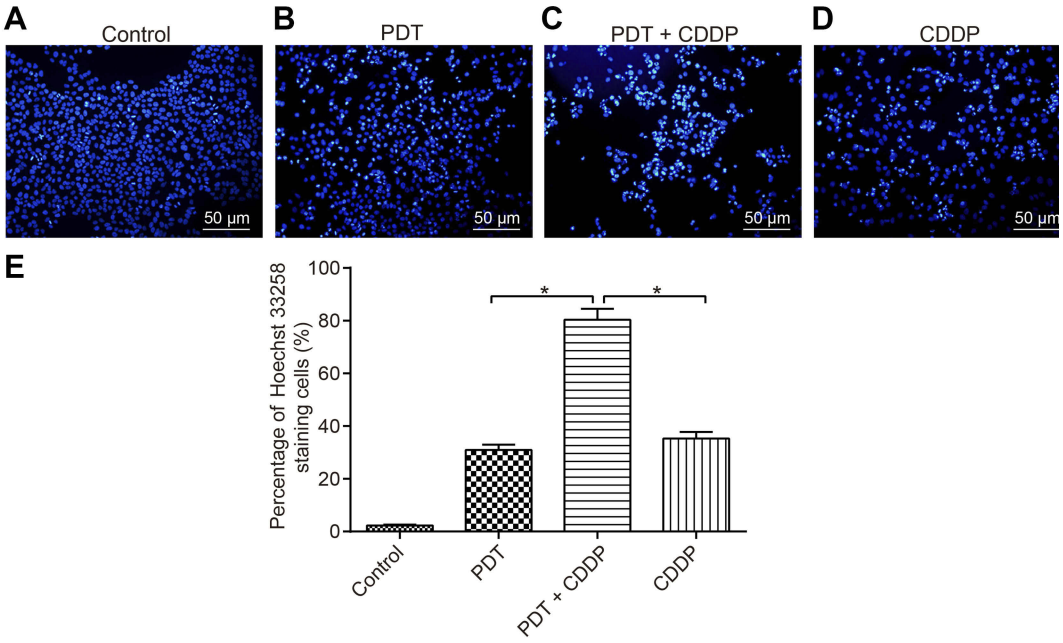

Figure 6 Hoechst 33258 staining of different cell groups. The blue areas stained by Hoechst 33258 represent nuclei. (**A**) Control group, (**B**) PDT group, (**C**) PDT+CDDP group, (**D**) CDDP groups. Scale bars represent 50 μm in all images. (**E**) Percentage of cells with deeply dyed nuclei. Values are expressed as the mean value ± SD, and the experiment was repeated in triplicate (*p<0.05).
Abbreviations: PDT, photodynamic therapy; CDDP, cisplatin.

Analysis of PD-L1 expression under different treatments

With accumulating evidence serving as the basis to support the vital role of PD-L1 in cancer, we investigated PD-L1 expression at the levels of gene and protein. RT-qPCR analysis showed that PDT treatment did not result in an increase in PD-L1 expression compared to the control group (Figure 8), whereas an increase in PD-L1 expression was evident due to 5 μM CDDP in comparison with the control group (p<0.05). Sequential treatment led to significant reduction in PD-L1 expression in comparison to the individual use of CDDP (p<0.05). Western blot analysis provided further evidence supporting these findings as illustrated in Figure 9.

Discussion

Platinum (Pt) compounds, including cisplatin, carboplatin, and oxaliplatin, have emerged as the most commonly used drugs for a wide spectrum of solid tumors.[21,22] The combined use of Pt compounds with radiotherapy and/or

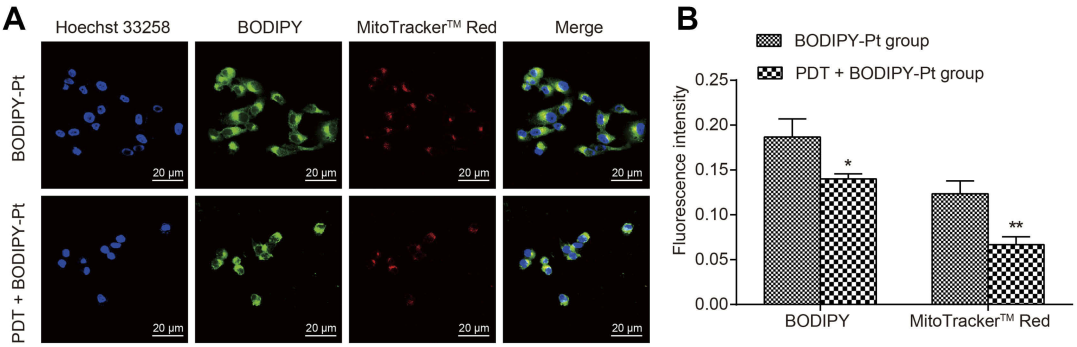

Figure 7 Confocal laser scanning analysis of mitochondrial pathway. (**A**) Upper panel represents BODIPY-Pt treatment group and lower panel represents the group treated by PDT followed by BODIPY-Pt. Both green and red spots, evoked from BODIPY and Mito Tracker™ Red, respectively, represent mitochondria, while the blue ones stained by Hoechst 33258 represent nuclei. Scale bars represent 20 μm in all images. (**B**) Analysis of fluorescence intensity which represents the amounts of mitochondria in BODIPY-Pt and PDT+BODIPY-Pt treatment group. Values are expressed as the mean fluorescence intensity ± SD, and the experiment was repeated in triplicate (*p<0.05).
Abbreviations: PDT, photodynamic therapy; BODIPY-Pt, 1,3,5,7-tetramethyl-8-(4-pyridyl)-4,4'-difluorobora-dia-zaindacene labeled platinum conjugate.

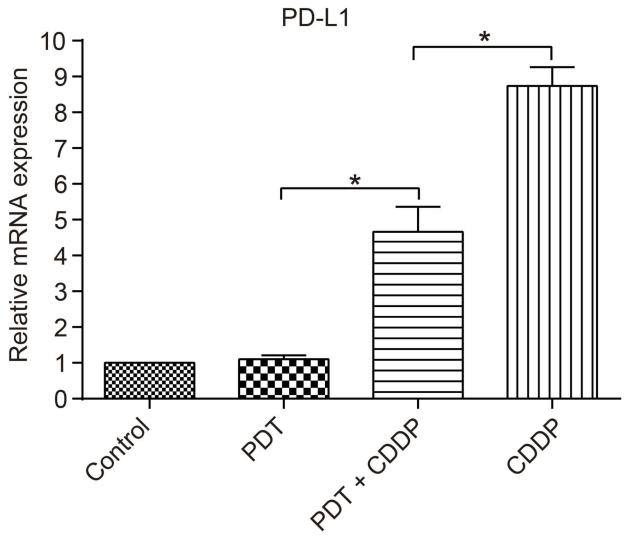

Figure 8 RT-qPCR analysis of PD-L1 expression in Hep-2 cells in different treatment groups. Data represent the mean value ± SD, and the experiment was repeated in triplicate (*p<0.05). The relative expression was obtained by normalizing to reference gene β-actin.
Abbreviations: PDT, photodynamic therapy; CDDP, cisplatin; PD-1, programmed death receptor-ligand 1; RT-qPCR, real-time quantitative polymerase chain reaction.

surgery has shown remarkable results in a number of advanced cancers and metastatic tumor cells.[23] The use of CDDP as a chemotherapeutic agent for treating various cancers such as head-and-neck squamous cell carcinoma (HNSCC), bladder, cervical, ovarian, testicular cancer, non-small cell lung cancer (NSCLC), and mesothelioma was approved several years ago by the US Food and Drug Administration for clinical use.[24]

Although Pt compounds are widely used, there is very little known on the underlying mechanisms involved. The action of Pt on DNA and further induction of cell apoptosis is the most widely accepted mechanism regarding the use of Pt in the treatment of tumor.[25,26] An existing research highlighted that Pt was predominantly localized in the mitochondria.[19] Previous studies have speculated the involvement of other targets in the action of Pt. The binding of CDDP to RNA results in the atypical cross-links of RNA, which is representative of a blockade for reverse transcription.[27–29] The ability of Pt to bind to several cellular proteins, including Hsp90, G-actin, and ubiquitin, resulted in alternation in normal biological function.[30–32]

However, with the usage of a number of the frontline chemotherapeutic drugs, such as CDDP, the development of drug resistance has been described.[33] Furthermore, severe side effects from CDDP have restricted the applicable dose. Existing literature has explored the capabilities of combination therapies with different drugs or different modalities in an attempt to combat drug resistance including the combination of chemotherapy and PDT.[13–15,34] PDT has been employed as a broad aspect therapeutic modality for the treatment of various malignancies, including head and neck tumors, skin tumors, and digestive system tumors. PDT only affects areas with the strongest light illumination, without systemic side effects. Restricted light penetration limits the depth of tumor destruction using PDT to 1 cm[35] Due to these limitations, PDT is depicted as an adjuvant therapy. Trials on numerous combination modalities have been proven to be successful for effective cell apoptosis with fewer side effects.[36,37]

Conjointly, the results of previous studies and the present study support the therapeutic effect of the combined use of

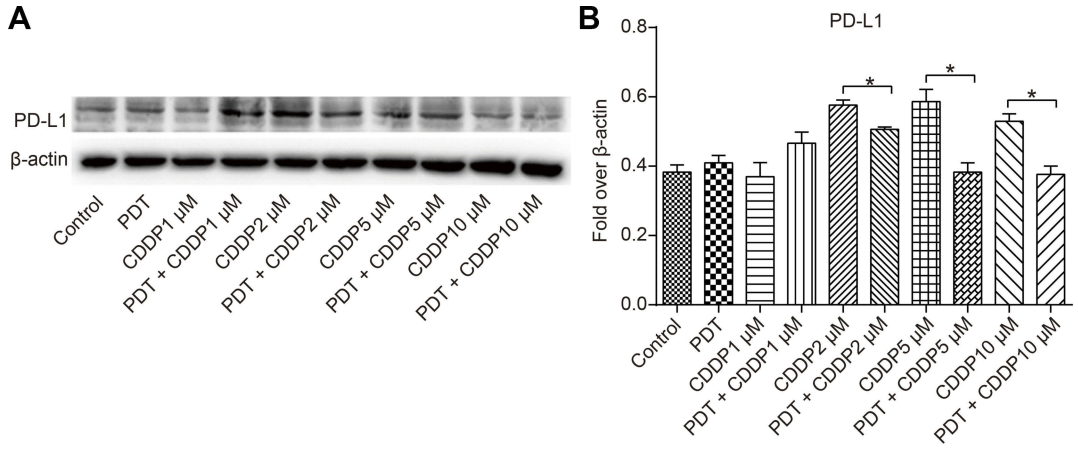

Figure 9 (**A**) Western blot of PD-L1 expression in Hep-2 cells in different treatment groups. (**B**) Analysis of Western blot of PD-L1 expression in Hep-2 cells in different treatment groups. Data represent the mean relative value ± SD, and the experiment was repeated in triplicate (*$p<0.05$).
Abbreviations: PDT, photodynamic therapy; CDDP, cisplatin; PD-1, programmed death receptor-ligand 1.

PDT and CDDP for efficacious synergistic apoptosis of tumor cells,[34,38] highlighting the use of a combination of PDT with low doses of CDDP as a superior alternative in contrast over the usage of high doses of CDDP independently. However, the sequential treatment modality with PDT followed by CDDP is yet to be identified. This treatment modality is much similar to the actual clinical practice that uses PDT and CDDP as therapeutic strategies, which has previously been investigated. The current study collected evidence supporting the synergistic effect of the sequential treatment modality of PDT followed by CDDP on both necrotic and apoptotic cell killing.

Drug resistance has been a persistent stumbling block, which has severely hindered the effectiveness of CDDP in clinical settings. Reports have implicated the mediation of tumor drug resistance due to various mechanisms, including the induction of autophagy and drug efflux.[3,37] Under stressful conditions during chemotherapy, autophagy is upregulated as a response to increase the catabolic lysis of excessive or unnecessary proteins and organelles essential for metabolic homeostasis and appropriate cell growth rate in different microenvironments.[3] Reports have highlighted that m-THPC-mediated PDT does not induce resistance to chemotherapy, radiotherapy, or PDT on human breast cancer cells in vitro, and further flagged PDT as a potential treatment modality to overcome classical drug resistance or escape pathways.[39,40] Our findings were consistent with the aforementioned reports supporting the functionality PDT as an inhibitor to significantly decrease the level of ATG-7 and the LC3-II/LC3-I ratio, therefore reducing autophagy.

Next, fluorescent BODIPY-Pt was employed so as to study the drug effect on the mitochondrial pathway, as CDDP is predominantly localized in the mitochondria. BODIPY-Pt damages tumor cells through induction of apoptosis via activation of various signal transduction pathways, such as DNA pathway and mitochondrial toxicity.[19] Our results show that PDT can decrease the numbers of mitochondria as shown in Figure 7, suggesting that PDT decreases the fluorescence of mitochondria marker Mito Tracker™ Red, consistent with a previous study.[41] In addition, the overlapping effects of sequential treatment of PDT followed by BODIPY-Pt procedure on mitochondria had a synergistic impact on Hep-2 cell apoptosis.

PD-L1 is a costimulatory molecule involved in T-cell inactivation by binding to PD1 (CD279) in an antigen-independent manner. The interaction between tumor-associated PD-L1 interacts with PD1 has an inhibitory effect on the cell-mediated antitumor immune responses by inducing T-cell energy and apoptosis.[42] Reports have highlighted the upregulation of PD-L1 expression due to chemotherapeutic drugs.[4,43,44] In the present study, we obtained evidence exhibiting that the sequential treatment modality with PDT and CDDP significantly reduced PD-L1 expression in Hep-2 cells, suggesting that the combination therapy may potentially boost the antitumor immune response through suppression of PD-L1 expression.

Conclusion

In conclusion, our results demonstrated that the sequential treatment of m-THPC-based PDT followed by chemotherapy with CDDP augmented the efficacy of cell apoptosis in vitro, with the cumulative effect of apoptosis, necrosis, mitochondrial destruction, reduced autophagy, and attenuated PD-L1

expression. Therefore, the findings from our study provide insight for an alternative therapeutic pathway to treat cancer, with fewer adverse reactions. Although our study is the first to thoroughly investigate the efficacy and mechanisms of sequential treatment using PDT and CDDP in vitro, more studies are required for further validation of our findings.

Acknowledgments

We would like to acknowledge the Central Lab of the Second Hospital of Jilin University for providing the instruments and services and Professor Zhigang Xie for providing BODIPY-Platinum conjugates.

This work is supported by grants from the National Natural Science Youth Foundation of China (81502348), the National Natural Science Foundation of China (81572653), the International Cooperation Project from Science and Technology Department of Jilin Province (20180414054GH), the Natural Science Foundation of Jilin Province (20190201212JC), and the Bethune Project of Jilin University (470110000669).

Disclosure

The authors have declared that they have no conflicts of interest in regard to this work.

References

1. Zheng HG. The molecular mechanisms of chemoresistance in cancers. *Oncotarget*. 2017;8(35):59950–59964. doi:10.18632/oncotarget.19048
2. Ren F, Shen J, Shi H, et al. Novel mechanisms and approaches to overcome multidrug resistance in the treatment of ovarian cancer. *Biochim Biophys Acta*. 2016;1866(2):266–275. doi:10.1016/j.bbcan.2016.10.001
3. Sui X, Chen R, Wang Z, et al. Autophagy and chemotherapy resistance: a promising therapeutic target for cancer treatment. *Cell Death Dis*. 2013;4:e838.
4. Peng J, Hamanishi J, Matsumura N, et al. Chemotherapy induces programmed cell death-ligand 1 overexpression via the nuclear factor-kappab to foster an immunosuppressive tumor microenvironment in ovarian cancer. *Cancer Res*. 2015;75(23):5034–5045.
5. Mancuso MR, Massarweh SA. Endocrine therapy and strategies to overcome therapeutic resistance in breast cancer. *Curr Probl Cancer*. 2016;40(2–4):95–105.
6. Bourguignon LY, Earle C, Shiina M. Activation of matrix hyaluronan-mediated cd44 signaling, epigenetic regulation and chemoresistance in head and neck cancer stem cells. *Int J Mol Sci*. 2017;18(9). pii: E1849.
7. Kim JK, Jeon HY, Kim H. The molecular mechanisms underlying the therapeutic resistance of cancer stem cells. *Arch Pharm Res*. 2015;38 (3):389–401.
8. Lu HP, Chao CC. Cancer cells acquire resistance to anticancer drugs: an update. *Biomed J*. 2012;35(6):464–472.
9. Nowis D, Makowski M, Stoklosa T, et al. Direct tumor damage mechanisms of photodynamic therapy. *Acta Biochim Pol*. 2005;52(2):339–352.
10. Brodin NP, Guha C, Tome WA. Photodynamic therapy and its role in combined modality anticancer treatment. *Technol Cancer Res Treat*. 2015;14(4):355–368. doi:10.1177/1533034614556192
11. Hatz S, Lambert JD, Ogilby PR. Measuring the lifetime of singlet oxygen in a single cell: addressing the issue of cell viability. *Photochem Photobiol Sci*. 2007;6(10):1106–1116. doi:10.1039/b707313e
12. Hananya N, Green O, Blau R, Satchi-Fainaro R, Shabat D. A highly efficient chemiluminescence probe for the detection of singlet oxygen in living cells. *Angew Chem Int Ed Engl*. 2017;56(39):11793–11796. doi:10.1002/anie.201705803
13. van Straten D, Mashayekhi V, de Bruijn HS, Oliveira S, Robinson DJ. Oncologic photodynamic therapy: basic principles, current clinical status and future directions. *Cancers (Basel)*. 2017;9 (2). doi:10.3390/cancers9020019
14. Olivo M, Bhuvaneswari R, Lucky SS, Dendukuri N, Soo-Ping Thong P. Targeted therapy of cancer using photodynamic therapy in combination with multi-faceted anti-tumor modalities. *Pharmaceuticals (Basel)*. 2010;3(5):1507–1529. doi:10.3390/ph3051507
15. Postiglione I, Chiaviello A, Palumbo G. Enhancing photodynamyc therapy efficacy by combination therapy: dated, current and oncoming strategies. *Cancers (Basel)*. 2011;3(2):2597–2629. doi:10.3390/cancers3022597
16. Separovic D, Joseph N, Breen P, et al. Combining anticancer agents photodynamic therapy and lcl85 leads to distinct changes in the sphingolipid profile, autophagy, caspase-3 activation in the absence of cell death, and long-term sensitization. *Biochem Biophys Res Commun*. 2011;409(3):372–377. doi:10.1016/j.bbrc.2011.04.091
17. Separovic D, Breen P, Boppana NB, et al. Increased killing of sccvii squamous cell carcinoma cells after the combination of pc 4 photodynamic therapy and dasatinib is associated with enhanced caspase-3 activity and ceramide synthase 1 upregulation. *Int J Oncol*. 2013;43 (6):2064–2072. doi:10.3892/ijo.2013.2132
18. Zhou XQ, Meng LB, Huang Q, et al. Synthesis and in vitro anticancer activity of zinc(ii) phthalocyanines conjugated with coumarin derivatives for dual photodynamic and chemotherapy. *ChemMedChem*. 2015;10(2):304–311. doi:10.1002/cmdc.201402401
19. Sun T, Guan X, Zheng M, Jing X, Xie Z. Mitochondria-localized fluorescent bodipy-platinum conjugate. *ACS Med Chem Lett*. 2015;6 (4):430–433. doi:10.1021/acsmedchemlett.5b00041
20. Crescenzi E, Chiaviello A, Canti G, et al. Low doses of cisplatin or gemcitabine plus photofrin/photodynamic therapy: disjointed cell cycle phase-related activity accounts for synergistic outcome in metastatic non-small cell lung cancer cells (h1299). *Mol Cancer Ther*. 2006;5(3):776–785. doi:10.1158/1535-7163.MCT-05-0425
21. Zhang J, Wang L, Xing Z, et al. Status of bi- and multi-nuclear platinum anticancer drug development. *Anticancer Agents Med Chem*. 2010;10(4):272–282. doi:10.2174/187152010791162270
22. Kanat O, Ertas H, Caner B. Platinum-induced neurotoxicity: a review of possible mechanisms. *World J Clin Oncol*. 2017;8(4):329–335. doi:10.5306/wjco.v8.i4.329
23. Kelland L. The resurgence of platinum-based cancer chemotherapy. *Nat Rev Cancer*. 2007;7(8):573–584. doi:10.1038/nrc2167
24. Hato SV, Khong A, de Vries IJ, Lesterhuis WJ. Molecular pathways: the immunogenic effects of platinum-based chemotherapeutics. *Clin Cancer Res*. 2014;20(11):2831–2837. doi:10.1158/1078-0432.CCR-13-3141
25. Todd RG, Lippard SJ. Inhibition of transcription by platinum antitumor compounds. *Metallomics*. 2009;1(4):280–291. doi:10.1039/b907567d
26. Jamieson ER, Lippard SJ. Structure, recognition, and processing of cisplatin-DNA adducts. *Chem Rev*. 1999;99(9):2467–2498.
27. Hostetter AA, Osborn MF, DeRose VJ. Rna-pt adducts following cisplatin treatment of saccharomyces cerevisiae. *ACS Chem Biol*. 2012;7(1):218–225.
28. Chapman EG, DeRose VJ. Enzymatic processing of platinated rnas. *J Am Chem Soc*. 2010;132(6):1946–1952.

29. Hostetter A, Chapman EG, DeRose VJ. Rapid cross-linking of an rna internal loop by the anticancer drug cisplatin. *J Am Chem Soc*. 2009;131(26):9250–9257.
30. Williams JP, Phillips HI, Campuzano I, Sadler PJ. Shape changes induced by n-terminal platination of ubiquitin by cisplatin. *J Am Soc Mass Spectrom*. 2010;21(7):1097–1106.
31. Ishida R, Takaoka Y, Yamamoto S, et al. Cisplatin differently affects amino terminal and carboxyl terminal domains of hsp90. *FEBS Lett*. 2008;582(28):3879–3883.
32. Zou J, An F, Liu G, Wang K. The binding of platinum (ii) complexes to rabbit skeletal muscle g-actin induces conformation changes. *Met Based Drugs*. 1995;2(4):233–240.
33. Galluzzi L, Vitale I, Michels J, et al. Systems biology of cisplatin resistance: past, present and future. *Cell Death Dis*. 2014;5:e1257.
34. Biteghe FN, Davids LM. A combination of photodynamic therapy and chemotherapy displays a differential cytotoxic effect on human metastatic melanoma cells. *J Photochem Photobiol B*. 2017;166:18–27.
35. Agostinis P, Berg K, Cengel KA, et al. Photodynamic therapy of cancer: an update. *CA Cancer J Clin*. 2011;61(4):250–281.
36. Chen YS, Peng YB, Yao M, et al. Cisplatin and photodynamic therapy exert synergistic inhibitory effects on small-cell lung cancer cell viability and xenograft tumor growth. *Biochem Biophys Res Commun*. 2017;487 (3):567–572.
37. Ali S, Khurshid A, Maqsood M, et al. Study of low doses cisplatin synergistic effect on photodynamic outcome of aluminum phythalocyanine on soft tissue sarcoma (rd) cell line. *Photodiagnosis Photodyn Ther*. 2015;12(1):146–149.
38. Nonaka Y, Nanashima A, Nonaka T, et al. Synergic effect of photodynamic therapy using talaporfin sodium with conventional anticancer chemotherapy for the treatment of bile duct carcinoma. *J Surg Res*. 2013;181(2):234–241.
39. Hornung R, Walt H, Crompton NE, et al. M-thpc-mediated photodynamic therapy (pdt) does not induce resistance to chemotherapy, radiotherapy or pdt on human breast cancer cells in vitro. *Photochem Photobiol*. 1998;68(4):569–574.
40. Spring BQ, Rizvi I, Xu N, Hasan T. The role of photodynamic therapy in overcoming cancer drug resistance. *Photochem Photobiol Sci*. 2015;14(8):1476–1491.
41. Hilf R. Mitochondria are targets of photodynamic therapy. *J Bioenerg Biomembr*. 2007;39(1):85–89.
42. Sukari A, Nagasaka M, Al-Hadidi A, Lum LC. Cancer immunology and immunotherapy. *Anticancer Res*. 2016;36(11):5593–5606.
43. McDaniel AS, Alva A, Zhan T, et al. Expression of pdl1 (b7-h1) before and after neoadjuvant chemotherapy in urothelial carcinoma. *Eur Urol Focus*. 2016;1(3):265–268.
44. Katsuya Y, Horinouchi H, Asao T, et al. Expression of programmed death 1 (pd-1) and its ligand (pd-l1) in thymic epithelial tumors: impact on treatment efficacy and alteration in expression after chemotherapy. *Lung Cancer*. 2016;99:4–10.

Supplementary material

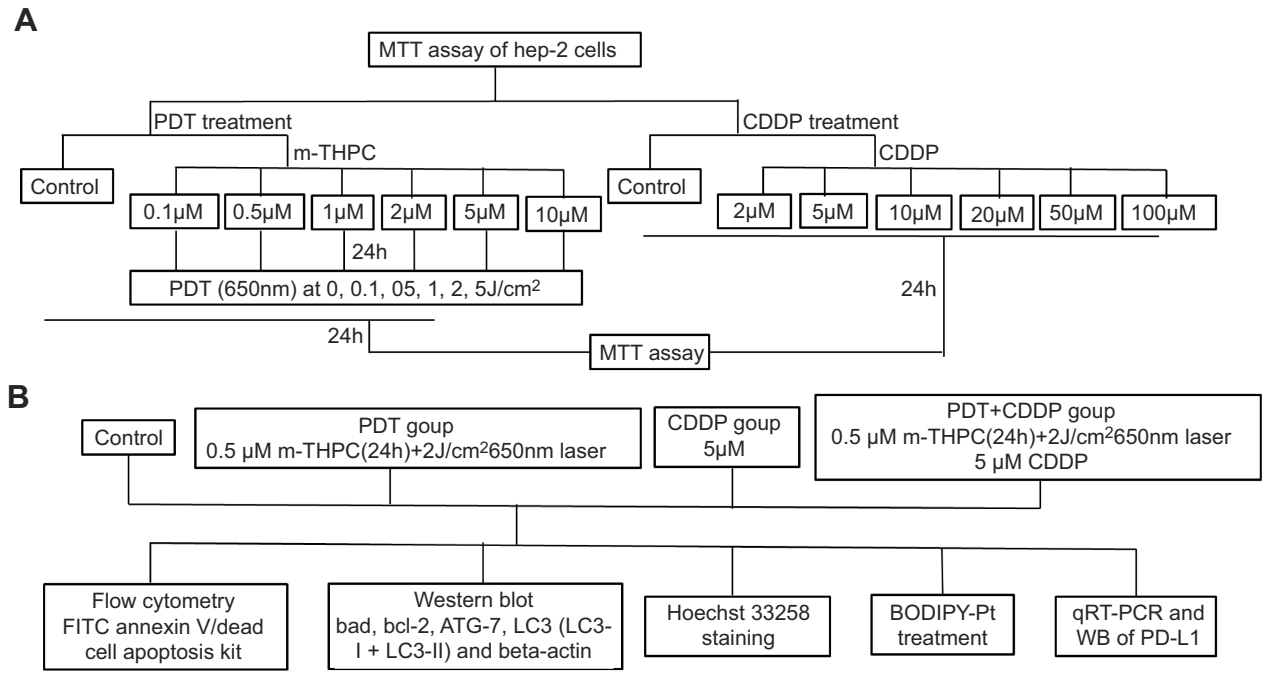

Figure S1 Visualization of experimental procedure. (**A**) Concentrations determination of m-THPC, CDDP, and laser energy dose for sequential treatment. (**B**) Experimental procedure of detection in the PDT, CDDP, and sequential treatment groups.

Abbreviations: BODIPY-Pt, CDDP, cisplatin; m-THPC, m-THPC, meta-Tetra (hydroxyphenyl) chlorin; MTT, 3-(4,5-Dimethylthiazol-2-yl)-2,5-diphenyltetrazolium bromide; PDT, photodynamic therapy; BODIPY-Pt, 1,3,5,7-tetramethyl-8-(4-pyridyl)-4,4'-difluorobora-dia-zaindacene labeled platinum conjugate; WB, Western blot.